Journal of Molecular Structure 1022 (2012) 197–203

Contents lists available at SciVerse ScienceDirect

Journal of Molecular Structure

journal homepage: www.elsevier.com/locate/molstruc

X-ray, FT-IR, NMR and PM5 structural studies and antibacterial activity of unexpectedly stable salinomycin–benzotriazole intermediate ester

Adam Huczyński [a,*], Jan Janczak [b], Michał Antoszczak [a], Joanna Stefańska [c], Bogumil Brzezinski [a]

[a] Faculty of Chemistry, A. Mickiewicz University, Grunwaldzka 6, 60-780 Poznań, Poland
[b] Institute of Low Temperature and Structure Research, Polish Academy of Sciences, PO Box 1410, 50-950 Wrocław, Poland
[c] Medical University of Warsaw, Department of Pharmaceutical Microbiology, Oczki 3, 02-007 Warsaw, Poland

HIGHLIGHTS

- Salinomycin–benzotriazole intermediate ester has been synthesised and characterised.
- X-ray, FT-IR, NMR and PM5 studies showed that ester exist in *O*–acyl form.
- The conversion of *O*–acyl form to *N*–oxide–*N*–acyl form is not observed.

ARTICLE INFO

Article history:
Received 13 April 2012
Received in revised form 7 May 2012
Accepted 7 May 2012
Available online 15 May 2012

Keywords:
Ionophores
Polyether antibiotics
Amide synthesis
HOBt intermediate
Anticancer drug
Molecular structure

ABSTRACT

The unexpectedly stable benzotriazole ester of salinomycin (SAL-HOBt) – an intermediate product of the amidation reaction of salinomycin has been isolated and structurally characterised (using a single crystal) by X-ray, FT-IR, NMR and semiempirical methods. The results of the X-ray and spectroscopic studies demonstrated that this intermediate ester exist in the solid state and in solution exclusively as the stable *O*–acyl form. The molecular structure of SAL-HOBt is stabilised by relatively weak intramolecular hydrogen bonds. The PM5 calculation of possible structures of SAL-HOBt has shown that the *O*–acyl form is more energetically favourable than its *N*–oxide–*N*–acyl isomers. The antimicrobial tests show that SAL-HOBt is active against Gram-positive bacteria and clinical isolates methicillin-resistant *Staphylococcus aureus* (MIC = 1–2 μg/ml).

1. Introduction

Salinomycin (Scheme 1) is a natural carboxylic polyether antibiotic isolated from *Streptomyces albus* [1]. Salinomycin and its salts exist in a pseudo-cyclic structure due to the formation of hydrogen bonds between the carboxylic group on the one side of the molecule and two hydroxyl groups on the opposite side [2]. Salinomycin, like other polyether antibiotics, is able to form complexes with monovalent cations (especially with K^+) and transport them across lipid membranes [3].

Recently it has been shown that salinomycin selectively kills breast cancer stem cells. [4] and it is considered to be a potential anti-cancer drug for cancer chemoprevention and cancer therapy [5].

In our previous papers we have described the synthesis of several amide derivatives of polyether ionophore – monensin A using one of the most popular methods of amides synthesis i.e. reaction between carboxylic acid and amines with addition of DCC (1,3-dicyclohexylcarbodiimide) and HOBt (1-hydroxybenzotriazole) which is a well-known acyl transfer agent in peptide synthesis [6–10].

On the basis of our previous experience we have performed synthesis of several amides of salinomycin. In one case, i.e. in the reaction between salinomycin acid and 1-naphthylamine at room temperature with the addition of DCC and HOBt, the expected amide product was not observed. Detailed analysis of the collected series of fractions from flash chromatography allowed us to discover an unexpected by-product (30% yield). This product is an active intermediate HOBt ester. Such esters, according to literature data have very interesting properties, i.e. they can exist in three forms shown in Scheme 2. The conversion of *O*–acyl form (A) to *N*–oxide–*N*–acyl isomer (B) has also been previously observed [11–17].

In this paper we report the synthesis and the structure elucidation of the novel benzotriazole active ester of salinomycin

* Corresponding author.
E-mail address: adhucz@amu.edu.pl (A. Huczyński).

0022-2860/$ - see front matter © 2012 Elsevier B.V. All rights reserved.
http://dx.doi.org/10.1016/j.molstruc.2012.05.019

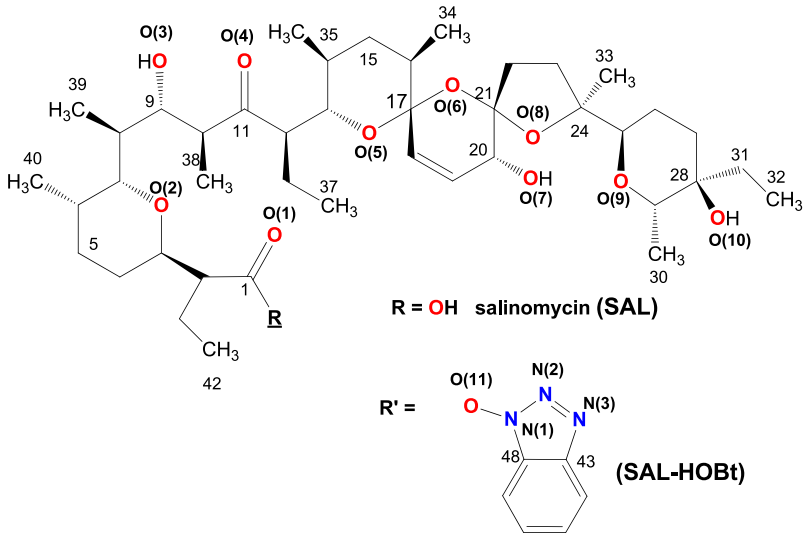

Scheme 1. The structures of salinomycin (SAL) and benzotriazole ester of salinomycin (SAL-HOBt).

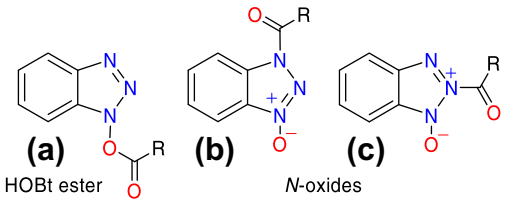

Scheme 2. The possible tautomers of HOBt ester.

(SAL-HOBt). The structures of SAL-HOBt in solid state and in solution were studied using X-ray diffraction, FT-IR and NMR spectroscopy as well as PM5 semi-empirical calculations and were discussed in detail.

The antimicrobial activity of SAL-HOBt is also determined and compared with that of unmodified salinomycin.

2. Experimental

DCC, HOBt and the solvents applied were commercial products of Sigma and were used without any further purification. The spectral–grade solvents were stored over 3 Å molecular sieves for several days. Handling of the compounds was performed in a carefully dried, CO_2-free glove box.

2.1. Isolation of salinomycin sodium salt (SAL-Na)

SAL-Na was isolated from Sacox® 120 microGranulate an anticoccidial feed additive distributed by Huvepharma Poland. 100 g of the permix was dissolved in dichloromethane. The solvent was evaporated under reduced pressure and the crude product obtained was purified by dry column vacuum chromatography (gradient solvent mixture hexane/CH_2Cl_2) giving 6 g pure SAL-Na. The spectroscopic data of SAL-Na are in agreement with the previously published assignments [3].

2.2. Synthesis of salinomycin acid (SAL)

SAL-Na was dissolved in dichloromethane and stirred vigorously with a layer of aqueous sulphuric acid (pH = 1.5). The organic layer containing SAL was washed with distilled water, and dichloromethane was evaporated under reduced pressure to dryness to produce the acid. The spectroscopic data of SAL are in agreement with the previously published assignments [18].

2.3. Preparation of SAL-HOBt

For the first time SAL-HOBt has been obtained as an unexpected by-product in the reaction between SAL and 1-naphthylamine but we developed also a synthetic procedure to obtain this compound.

A solution of salinomycin acid (1000 mg, 1.33 mmol), 1,3-dicyclohexylcarbodiimide (140 mg, 2.03 mmol) in dichloromethane and 1-hydroxybenzotriazole hydrate (200 mg, 1.46 mmol) dissolved in tetrahydrofuran were mixed and stirred at 0 °C for 1 h. After this time, the reaction mixture was stirred at room temperature for further 48 h. Then the solvents were distilled under reduced pressure to dryness. The residue was suspended in dichloromethane and filtered off to remove the by-product 1,3-dicyclohexylurea. The filtrate was evaporated under reduced pressure and purified by Dry Column Vacuum Chromatography on silica gel (Fluka type 60) to give SAL-HOBt as a colourless solid (45% yield). Pure compound SAL-HOBt was dissolved in warm acetonitrile. The solution was allowed to evaporate at room temperature. After several days the crystals were formed in 30% yield. The spectroscopic data and the exemplary NMR spectra are included in the Supplementary material (Figs. S1–S6).

2.4. X-ray measurements

Colourless single crystal of SAL-HOBt was used for data collection on a four-circle KUMA KM-4 diffractometer equipped with a two-dimensional CCD area detector. The graphite monochromatised Mo Kα radiation ($\lambda = 0.71973$ Å) and the ω scan technique ($\Delta\omega = 1°$) were used for data collection. Data collection and reduction along with absorption correction were performed using CrysAlis software package [19]. The structure was solved by direct methods using SHELXS-97 [20] revealing positions of almost all non-hydrogen atoms. The remaining atoms were located from subsequent difference Fourier syntheses. The structure was refined using SHELXL-97 [20] with the anisotropic thermal displacement parameters. The hydrogen atoms of the aromatic ring were refined with the riding model. The H atoms of CH_3, CH_2 and CH groups were constrained: $U_{iso} = 1.5U_{eq}$ of the C joined H and the C—H distance of 0.97 Å. Visualisation of the structure was made with the Diamond 3.0 program [21]. Details of the data collection

parameters, crystallographic data and final agreement parameters are given in Table 1. Selected geometrical parameters are listed in Table 2.

2.5. NMR measurements

The ^{1}H and ^{13}C NMR spectra of SAL-HOBt (0.07 mol dm^{-3}) were recorded in CD_3CN and CD_2Cl_2 solutions using a Bruker Avance 600 MHz spectrometer. All spectra were locked to deuterium resonance of CD_3CN or CD_2Cl_2. The ^{1}H NMR measurements were carried out at the operating frequency 600.0018 MHz and the ^{13}C NMR spectra at the operating frequency 150.885 MHz. The temperature 298.0 K and TMS as the internal standard were used in both cases. No window function or zero filling was used. The errors of the ^{1}H and ^{13}C NMR chemical shift values were 0.01 ppm and 0.1 ppm, respectively. The ^{1}H and ^{13}C NMR signals were assigned using 2-D (COSY, HETCOR, NOESY and HMBC) spectra whose examples are shown in the Supplementary Materials. 2-D spectra were recorded using standard pulse sequences from Bruker pulse-sequence libraries.

2.6. FT-IR measurements

In the mid infrared region the FT-IR spectra of SAL-HOBt were recorded in chloroform and acetonitrile solution (0.07 mol dm^{-3}) and potassium bromide in the form of KBr pellets. For solution a cell with Si windows and wedge-shaped layers was used to avoid interferences (mean layer thickness 170 μm). The spectra were taken with an IFS 113v FT-IR spectrophotometer (Bruker, Karlsruhe) equipped with a DTGS detector; resolution 2 cm^{-1}, NSS = 64. The Happ-Genzel apodization function was used.

2.7. PM5 semi-empirical calculation

PM5 quantum calculations were performed using the WinMopac 2007 program at the semi-empirical level (Cache Work System Pro Version 7.5.085 – Fujitsu) [22]. The PM5 quantum method is based on the use of the Schrödinger equation to determine bond strengths, atomic hybridisations, partial charges and orbitals from the positions of the atoms and the net charge. The initial structures for PM5 calculations were obtained from the molecular mechanics (MM3) calculations (WinMopac 2007). The MM3 optimisations of salinomycin parts in the structures of form B and C of SAL-HOBt were performed after removing benzotriazole substituent in *O*-acyl form of SAL-HOBt (form A) determined from the X-ray analysis and replacing it by the benzotriazole substituents in form B and C, respectively. The conformers of SAL-HOBt (A, B, and C) form characterised by the lowest energy, obtained from MM calculations were further optimised by the PM5 method at semi-empirical level with energy gradient not exceeding 42 kJ mol^{-1} at one step.

Table 1
Crystal data of SAL-HOBt · CH_3CN.

$C_{48}H_{75}N_3O_{11}\cdot CH_3CN$	D_x = 1.179 Mg m^{-3}
M_r = 911.16	D_m = 1.17 Mg m^{-3}, D_m measured by floatation
Orthorhombic, $P2_12_12_1$	MoKα radiation, λ = 0.71073 Å
a = 11.1018(6) Å	θ = 2.6–27.0°
b = 11.8135(6) Å	μ = 0.08 mm^{-1}
c = 39.133(2) Å	T = 295 K
V = 5132.4(5) Å^3	0.37 × 0.28 × 0.22 mm, Parallelepiped, colourless
Z = 4	$R[F^2 > 2\sigma(F^2)]$ = 0.0803, $wR(F^2)$ = 0.1859
$F(000)$ = 1976	S = 1.032, Flack parameter: 0.29(17)

Table 2
Selected geometrical parameters (Å, °).

C1—O1	1.171(7)	C1—O11	1.418(7)	C3—O2	1.435(6)
C7—O2	1.439(6)	C9—O3	1.433(6)	C11—O4	1.216(6)
C13—O5	1.446(6)	C17—O5	1.456(5)	C17—O6	1.396(6)
C20—O7	1.430(6)	C21—O6	1.442(6)	C21—O8	1.402(6)
C24—O8	1.457(6)	C29—O9	1.444(6)	C25—O9	1.452(6)
C28—O10	1.433(7)	C1—C2	1.517(8)	C2—C3	1.548(8)
C3—C4	1.526(8)	C4—C5	1.522(8)	C5—C6	1.514(9)
C6—C7	1.537(8)	C7—C8	1.535(8)	C8—C9	1.530(7)
C9—C10	1.525(7)	C10—C11	1.527(7)	C11—C12	1.513(7)
C12—C13	1.542(6)	C13—C14	1.534(6)	C14—C15	1.512(7)
C15—C16	1.524(8)	C16—C17	1.525(7)	C17—C18	1.499(7)
C18—C19	1.396(4)	C19—C20	1.475(7)	C20—C21	1.509(7)
C21—C22	1.517(7)	C22—C23	1.528(7)	C23—C24	1.541(7)
C24—C25	1.524(7)	C25—C26	1.513(7)	C26—C27	1.532(8)
C27—C28	1.530(8)	C28—C29	1.539(7)	C29—C30	1.530(7)
C31—C32	1.553(9)	C28—C31	1.509(8)	C36—C37	1.523(7)
C41—C42	1.519(9)	O11—N1	1.386(7)	N1—N2	1.383(8)
N2—N3	1.310(9)	N3—C43	1.378(10)	N1—C48	1.338(10)
O1—C1—O11		121.2(6)	C3—O2—C7		116.1(4)
C13—O5—C17	115.8(4)		C17—O6—C21		120.7(4)
C21—O8—C24	112.0(4)		C29—O9—C25		114.7(4)

2.8. Antimicrobial activity

The micro-organisms used in the tests were the following: Gram-positive cocci: *Staphylococcus aureus* NCTC 4163, *S. aureus* ATCC 25923, *S. aureus* ATCC 6538, *S. aureus* ATCC 29213, *Staphylococcus epidermidis* ATCC 12228, *S. epidermidis* ATCC 35984, Gram-negative rods: *Escherichia coli* ATCC 10538, *E. coli* ATCC 25922, *E. coli* NCTC 8196, *Proteus vulgaris* NCTC 4635, *Pseudomonas aeruginosa* ATCC 15442, *P. aeruginosa* NCTC 6749, *P. aeruginosa* ATCC 27853, *Bordetella bronchiseptica* ATCC 4617 and yeasts-like organisms: *Candida albicans* ATCC 10231, *C. albicans* ATCC 90028, *Candida parapsilosis* ATCC 22019. Hospital strains of *S. aureus* were isolated from different biological materials of patients of the Warsaw Medical University Hospital. Ten of these strains were methicillin-resistant *Staphylococcus* (MRSA) and ten other strains were methicillin-sensitive *S. aureus* (MSSA). The other micro-organisms used here were provided by the Department of Pharmaceutical Microbiology, Medical University of Warsaw, Poland.

Antimicrobial activity was examined by the disc-diffusion method under standard conditions using Mueller–Hinton II agar medium (Becton Dickinson) for bacteria and RPMI agar with 2% glucose (Sigma) according to CLSI (previously NCCLS) guidelines [24].

Sterile filter paper discs (9 mm diameter, Whatman No. 3 chromatography paper) were dripped with tested compound solutions (in MeOH or MeOH/DMSO 1:1) to load 400 μg of a given compound per disc. Dry discs were placed on the surface of appropriate agar medium. The results (diameter of the growth inhibition zone) were read after 18 h of incubation at 35 °C. Compounds with recognised activity in disc-diffusion tests were examined by the agar dilution method to determine their MIC – Minimal Inhibitory Concentration (CLSI) [25]. Concentrations of the agents tested in solid medium ranged from 3.125 to 400 μg/ml. The final inoculum of all studied organisms was 10^4 CFU ml^{-1} (colony forming units per ml). Minimal inhibitory concentrations were read after 18 h of

Table 3
Hydrogen-bond geometry (Å, °).

D—H···A	D—H	H···A	D···A	D—H···A
O3—H···O4	0.82	2.54	3.037(6)	120.4
O7—H···O9	0.88	2.08	2.963(5)	178.4
O10—H···O9	0.82	2.35	2.778(5)	113.0

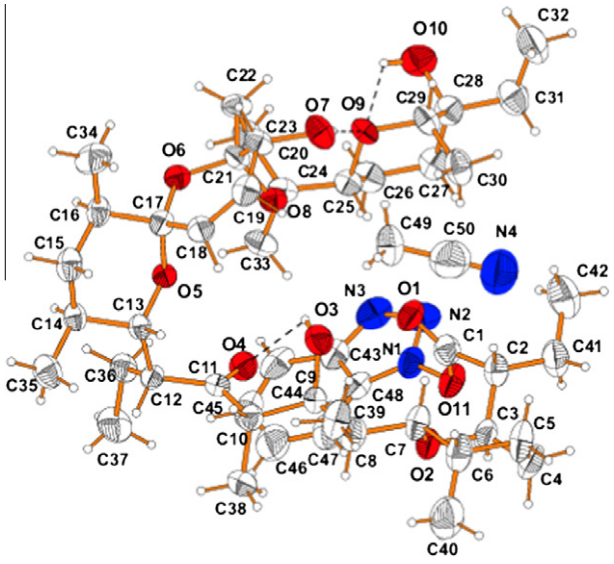

Fig. 1. View of the molecular structure of salinomycin HOBt ester acetonitrile solvate (SAL-HOBt·CH_3CN) with the atoms labelling. Dashed lines represent the hydrogen bonds.

incubation at 35 °C. The data concerning the antimicrobial activity of the compounds are summarised in Table 4.

3. Results and discussion

The structure and the numbering of the atoms of salinomycin and SAL-HOBt are shown in Scheme 1.

3.1. X-ray structure analysis

The crystallization of this compound from acetonitrile solution give fine SAL-HOBt·CH_3CN crystals whose structure was determined by single-crystal X-ray diffraction (Tables 1–3, Figs. 1 and 2) showing that in the solid state the intermediate ester SAL-HOBt existed only in the *O*–acyl form (Fig. 1). The absolute configuration of SAL-HOBt is (*2R*, *3R*, *6S*, *7R*, *8S*, *9S*, *10S*, *12R*, *13S*, *14S*, *16R*, *17R*, *20R*, *21S*, *24S*, *25R*, *28R*, *29S*) and it was analogously determined for salinomycin [1,2]. The molecule of SAL-HOBt, exhibits a pseudo-cyclic conformation of salinomycin. Within the crystal structure there are three intramolecular O—H···O hydrogen bonds (O7—H···O9, O10—H···O9 and O3—H···O4) resulting from the proximity of the hydroxyl groups (O7—H and O10—H) to the etheric oxygen atom O9 of negative polarity from the six-membered ring and the proximity of the hydroxyl group O3—H to the carbonyl oxygen O4 (Table 3). All six-membered rings of SAL-HOBt exhibit the chair conformation in which the bond lengths and angles do not differ significantly from the standard values (Table 2). The arrangement of molecules of SAL-HOBt is mainly determined by van der Waals forces, since there are no directional intermolecular interactions like hydrogen bonds. The solvent acetonitrile molecules are located in the crystal in the voids between the molecules of SAL-HOBt (Fig. 2).

3.2. Spectroscopic analysis

Hydroxybenzotriazole esters, according to literature data, can exist in three forms shown in Scheme 2, depending on the polarity of the solvent [11–17]. It has been reported that the ν(C=O) stretching vibration of the ester of HOBt depends on the measurement medium since the *N*–oxide–*N*–acyl form (isomer B) is favoured in polar solvents, while the desired active *O*–acyl form (isomer A) predominates in less-polar solvents [16,17]. Therefore, we checked which form of SAL-HOBt was present in the solid and in different solvents. The crystallization of this compound from acetonitrile solution give crystals whose structure is determined by X-ray method showing that in the crystal state the SAL-HOBt existed only in the *O*–acyl form (Fig. 1).

The FT-IR spectrum of crystalline SAL-HOBt·CH_3CN in KBr pellets (Fig. 3, solid line) shows a characteristic band at 1822 cm^{-1} assigned to ν(C=O) stretching vibration of the carbonyl group of the *O*–acyl form (Scheme 2., isomer A) [16,17]. To answer the question of what happens to the molecular structure of SAL-HOBt ester in the solution we performed a detail FT-IR and NMR investigation in two solvents: non-polar (dichloromethane) and polar (acetonitrile). In Fig. 3 the FT-IR spectra of SAL-HOBt in acetonitrile (dashed line) and in dichloromethane (dashed-dotted line), respectively, are compared with the FT-IR spectrum of crystalline SAL-HOBt

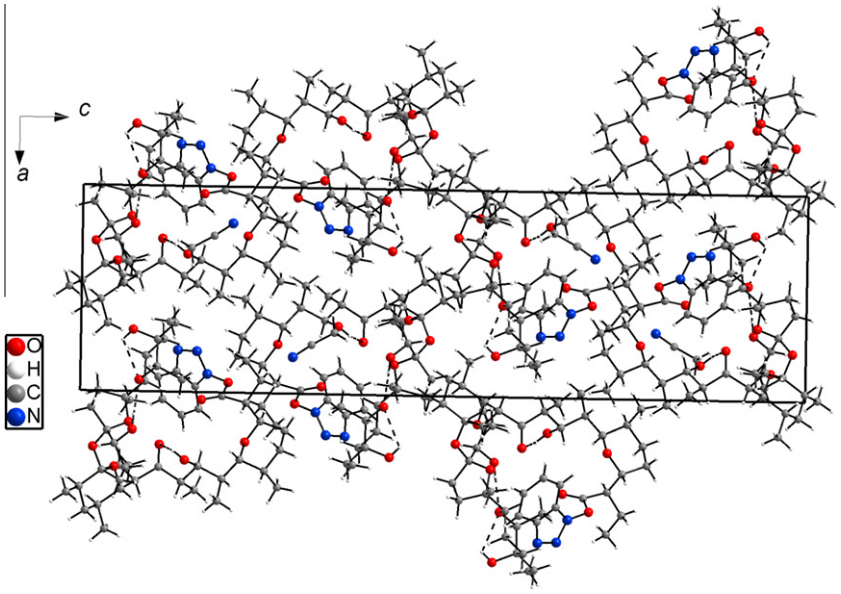

Fig. 2. Arrangement of SAL-HOBt·CH_3CN in the unit cell. Dashed lines represent the intramolecular O—H···O hydrogen bonds.

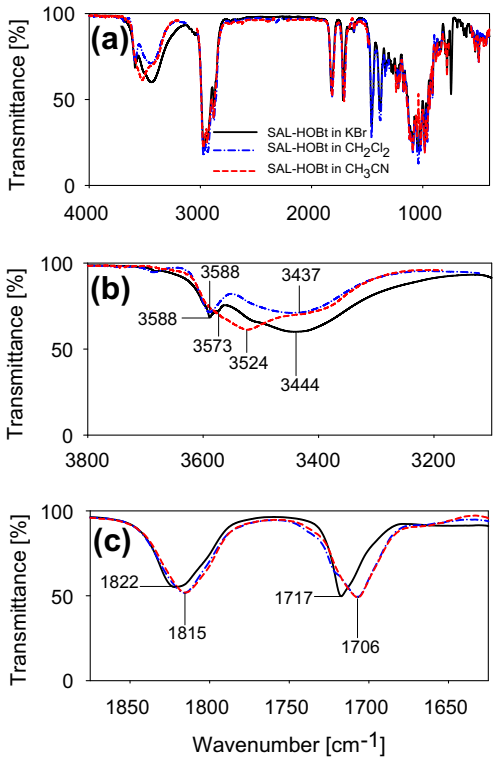

Fig. 3. The FT-IR spectra of: crystal of SAL-HOBt recorded in KBr pellet (—) and in solution acetonitrile (- - -) and dichloromethane (- · -): (a) 4000–400 cm^{-1}; (b) 3800–3100 cm^{-1}; (c) 1875–1625 cm^{-1}.

(solid line). Unexpectedly, the band assigned to the ν(C═O) vibration of the ester group in the solid does not disappear in the FT-IR spectra in both solutions indicating that the *O*–acyl form of SAL-HOBt is conserved. We also checked that this form is stable on long-term standing and on heating.

A comparison of the FT-IR spectra (Fig. 3) shows that the solution structure of SAL-HOBt is slightly different from its solid state structure. A shift of the band assigned to the ν(C═O) vibration of the ester group from 1822 cm^{-1} to 1815 cm^{-1} and a shift of the band assigned to the ν(C═O) vibration of the ketone group from 1717 cm^{-1} to 1706 cm^{-1} indicate that these groups are slightly stronger engaged in the hydrogen bonds in the solutions. This conclusion is confirmed by the changes in the bands assigned to the ν(O—H) vibrations as shown in Fig. 3b and by changes in the position of OH signals in ^{1}H NMR spectra of SAL-HOBt as shown in Fig. 4.

The ^{13}C NMR signal assigned to C(1) atom of SAL-HOBt is observed at 171.1 ppm and 172.2 ppm in CD_2Cl_2 and CD_3CN, respectively. This upfield chemical shift of this atom is caused by the electron-donating mesomeric effect within the HOBt ester. The ^{1}H and ^{13}C NMR, HETCOR, COSY, NOESY and especially the HMBC spectra (all included in the Supplementary material, Figs. S1–S6) as well as the FT-IR spectra in two solutions and in solid state clearly show that SAL-HOBt exists exclusively in the *O*–acyl form.

3.3. Semiempirical calculation

The heat of formation (HOF) of the lowest-energy structures calculated using PM5 semiempirical method of three possible forms of SAL-HOBt shown in Scheme 2 are presented together with the their molecular structures in Fig. 5. The calculated HOF values indicate that generally the structure of type A (*O*–acyl form (A)) is more energetically favourable than the corresponding *N*–oxide–*N*–acyl type (isomers B and C) which is in agreement with the X-ray, NMR and FT-IR data. It is also interesting to note that the type B structure is energetically preferred over C of the *N*–oxide–*N*–acyl form.

The compared structures of three types (isomers A, B and C) of SAL-HOBt calculated by PM5 semiempirical method are shown in Fig. 5. The comparison of these structures indicates that three OH groups of SAL-HOBt molecule in all types (A, B and C) are engaged to a similar degree in the intramolecular hydrogen bonds. Therefore, irrespective of the type of structural form of benzotriazole substituent, the molecular structure of salinomycin part of the SAL-HOBt molecule is similar.

3.4. Antimicrobial activity

The antimicrobial activities of salinomycin (SAL) and its benzotriazoli ester derivatives (SAL-HOBt) were studied *in vitro* against the typical Gram-positive cocci, Gram-negative rods and yeast-like organisms as well as against a series of clinical isolates of *Staphylococcus*: methicillin-resistant *S. aureus* (MRSA) and methicillin-sensitive *S. aureus* (MSSA). Hospital strains of methicillin-resistant *Staphylococcus* were isolated from different biological materials of patients from the Warsaw Medical University Hospital.

The data concerning the antimicrobial activity of the compounds are summarised in Table 4. Both SAL and SAL-HOBt exhibited relatively high activity against standard strains of *S. epidermidis and S. aureus* and showed relatively high activity against the series of clinical isolates methicillin-resistant *S. aureus* (MRSA) and methicillin-sensitive *S. aureus* (MSSA). For most clinical *Staphylococcus* the minimum inhibitory concentration (MIC)

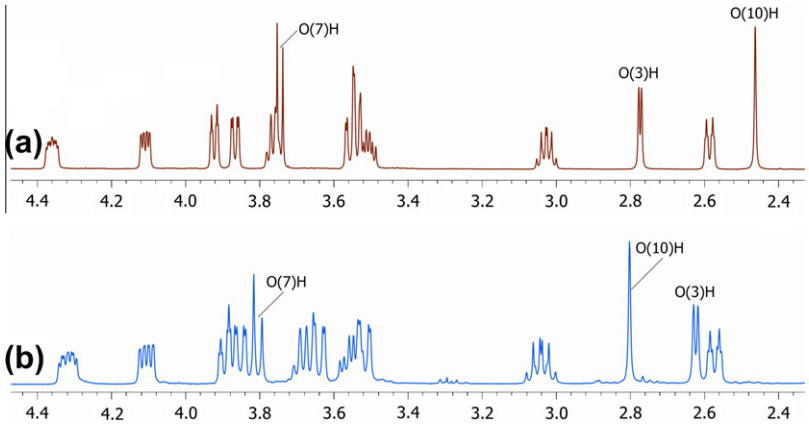

Fig. 4. ^{1}H NMR spectra in the region of OH proton signals of SAL-HOBt recorded in: (a) CD_2Cl_2 and (b) CD_3CN.

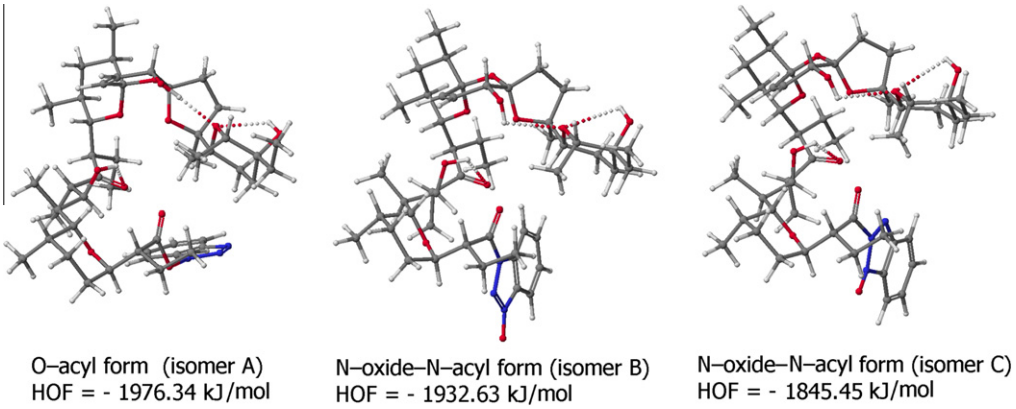

Fig. 5. Comparison of the structures of tree possible isomers of SAL-HOBt calculated using the PM5 semiempirical method.

Table 4
Antibacterial activity of salinomycin (SAL) and ester with 1-hydroxybenzotriazole (SAL-HOBt) against Gram-positive bacteria and hospital strains methicillin-resistant *Staphylococcus aureus* and methicillin-sensitive *Staphylococcus aureus* (MIC (μg/ml)) [25,26].

	SAL	SAL-HOBt
Typical strains of Gram-positive bacteria		
S. aureus NCTC 4163	2	8
S. aureus ATCC 25923	2	16
S. aureus ATCC 6538	2	16
S. aureus ATCC 29213	2	16
S. epidermidis ATCC 12228	2	8
S. epidermidis ATCC 35984	2	16
Hospital strains of methicillin-resistant Staphylococcus aureus (MRSA)		
S. aureus 393/10	2	4
S. aureus 394/10	2	4
S. aureus 399/10	1	2
S. aureus 400/10	1	1
S. aureus 401/10	1	2
S. aureus 450/11	2	4
S. aureus 451/11	2	4
S. aureus 452/11	1	2
S. aureus 481/11	1	2
S. aureus 482/11	2	2
Hospital strains of methicillin-sensitive Staphylococcus aureus (MSSA)		
S. aureus 440/11	1	2
S. aureus 441/11	2	2
S. aureus 442/11	2	2
S. aureus 443/11	2	2
S. aureus 444/11	2	2
S. aureus 445/11	1	2
S. aureus 446/11	1	2
S. aureus 447/11	2	4
S. aureus 448/11	2	2
S. aureus 449/11	1	2

values of SAL-HOBt were 1–4 μg/ml. This high antibacterial activity against MRSA is very important because MRSA are the most important epidemiological problems of contemporary hospital medicine. MRSA have become one of the key pathogens responsible for the increasingly troublesome hospital infections worldwide [27].

4. Conclusion

For the first time the ester intermediate formed between salinomycin acid and HOBt in the presence of DCC has been synthesised and its structure and behaviour in different solvents has been studied showing that its *O*–acyl form is preferred both in the crystal and the solution independently of the polarity of the solvent used.

Taking into account the X-ray, NMR and FT-IR data, the lowest-energy structure of a new benzotriazole derivative of salinomycin has been calculated and visualised by PM5 method indicating that the structure SAL-HOBt is stabilised by rather weak intramolecular hydrogen bonds, in agreement with the ^{1}H NMR and FT-IR spectroscopic data. The PM5 calculation of possible structures of SAL-HOBt has shown that the *O*–acyl form is more energetically favourable than its *N*–oxide–*N*–acyl isomers.

The antimicrobial tests have shown that SAL-HOBt derivative is a very active compound against the typical Gram-positive cocci as well as against a series of clinical isolates of *Staphylococcus*: methicillin-resistant *S. aureus* (MRSA) and methicillin-sensitive *S. aureus* (MSSA).

Appendix A. Supplementary material

Details on data collection and refinement, fractional atomic coordinates, anisotropic displacement parameters and full list of bond lengths and angles in CIF format have been deposited at the Cambridge Crystallographic Data Centre, No. CCDC 865744. Copies of this information may be obtained free of charge from The Director, CCDC, 12 Union Road, Cambridge, CB2 1EZ, UK (fax: +44 1223 336 033; email: deposit@ccdc.cam.ac.uk or http://www.ccdc.cam.ac.uk). Supplementary data (exemplary NMR) associated with this article can be found, in the online version, at http://dx.doi.org/10.1016/j.molstruc.2012.05.019.

References

[1] H. Kinashi, N. Otake, H. Yonehara, Tetrahedron Lett. 49 (1973) 4955.
[2] E.F. Paulus, M. Kurz, H. Matter, L. Vértesy, J. Am. Chem. Soc. 120 (1998) 8209.
[3] S. Mronga, G. Müller, J. Fischer, F. Riddell, J. Am. Chem. Soc. 115 (1993) 8414.
[4] P.B. Gupta, T.T. Onder, G. Jiang, K. Tao, C. Kuperwasser, R.A. Weinberg, E.S. Lander, Cell 138 (2009) 645.
[5] A. Huczynski, Chem. Biol. Drug Des. 79 (2012) 235.
[6] D. Łowicki, A. Huczyński, M. Ratajczak-Sitarz, A. Katrusiak, J. Stefańska, B. Brzezinski, F. Bartl, J. Mol. Struct. 923 (2009) 53.
[7] D. Łowicki, A. Huczyński, J. Stefańska, B. Brzezinski, Tetrahedron 65 (2009) 7730.
[8] D. Łowicki, A. Huczyński, J. Stefańska, B. Brzezinski, Tetrahedron 67 (2011) 1468.
[9] D. Łowicki, A. Huczyński, J. Stefańska, B. Brzezinski, Eur. J. Med. Chem. 45 (2010) 4050.
[10] D. Łowicki, A. Huczyński, B. Brzezinski, F. Bartl, J. Mol. Struct. 990 (2011) 121.
[11] K.A. Mahmoud, Y.-T. Long, G. Schatte, H.-B. Kraatz, Europ. J. Inorg. Chem. 1 (2005) 173.
[12] J. Singh, R. Fox, M. Wong, T.P. Kissick, J.L. Moniot, J.Z. Gougoutas, M.F. Malley, O. Kocy, J. Org. Chem. 53 (1988) 205.
[13] D.G. McCarthy, A.F. Hegarty, B.J. Hathaway, J. Chem. Soc. Perkin Trans. 2 (2) (1977) 224.
[14] D.G. McCarthy, A.F. Hegarty, J. Chem. Soc. Perkin Trans. 2 (2) (1977) 231.
[15] R. Bosch, G. Jung, W. Winter, Acta Cryst. C39 (1983) 1089.
[16] W. König, R. Geiger, Chemische Berichte 103 (1970) 788.

[17] K. Horiki, Tetrahedron Lett. 22 (1977) 1987.
[18] J. Ivanova, I.N. Pantcheva, M. Mitewa, S. Simova, M. Tanabe, K. Osakada, Chem. Centr. J. 5 (2011) (art. no. 52).
[19] CrysAlis CCD and CrysAlis Red program, Ver. 171.32.6, Oxford Diffraction Poland, Wrocław, Poland, 2006.
[20] G.M. Sheldrick, SHELXS97, SHELXL97, Programs for Crystal Structure Solution and Refinement, University of Göttingen, Göttingen, Germany, 1997.
[21] K. Brandenburg, K. Putz, Diamond, Ver. 3.0, Crystal and Molecular Structure Visualization, University of Bonn, Germany, 2006.
[22] Cache Work System Pro Version 7.5.085 UserGuide, Fujitsu, Beaverton, Oregon, USA, 2007.
[24] P. Przybylski, A. Huczyński, B. Brzezinski, J. Mol. Struct. 826 (2007) 156.
[25] Clinical and Laboratory Standards Institute. Performance Standards for Antimicrobial Disc Susceptibility Tests; Approved Standard M2-A9, Clinical and Laboratory Standards Institute, Wayne, PA, USA, 2006.
[26] Clinical and Laboratory Standards Institute. Methods for Dilution Antimicrobial Susceptibility Tests for Bacteria That Grow Aerobically; Approved Standard M7–A7, Clinical and Laboratory Standards Institute, Wayne, PA, USA, 2006.
[27] M. Bigos, A. Denys, Int. Rev. Allergol. Clin. Immunol. 14 (2008) 101.